

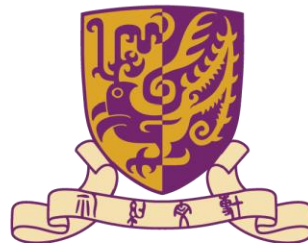
Searching light sterile neutrino in large-scale structures

Arxiv: 2501.16908 (JCAP06(2025)014)

Department of Physics, CUHK

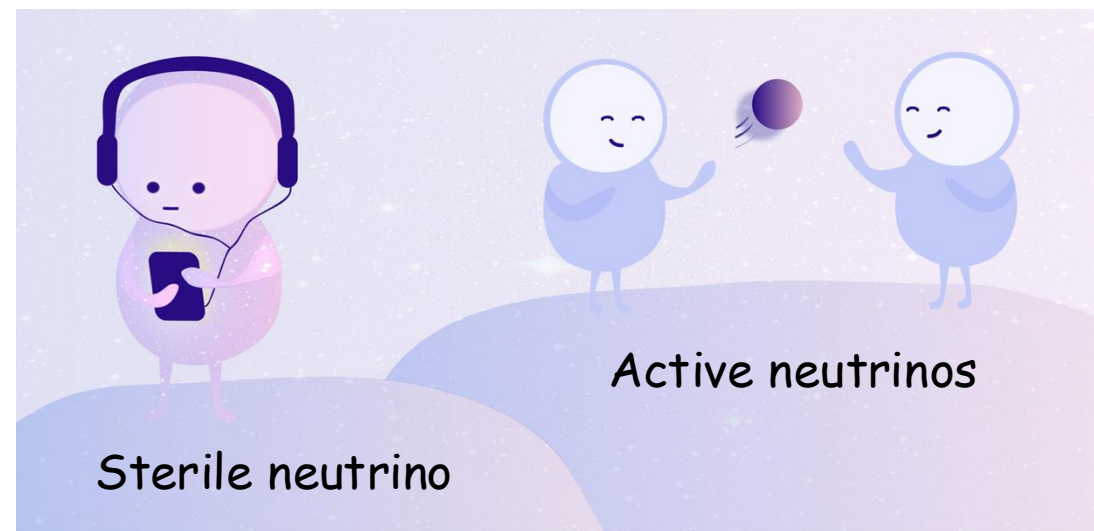
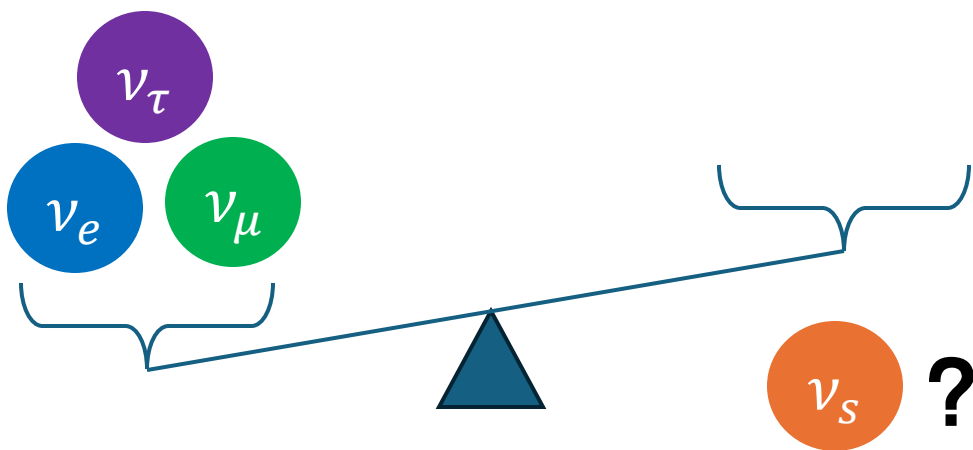
Rui Hu,

In collaboration with Ming-chung Chu, Wangzheng Zhang, Shek Yeung



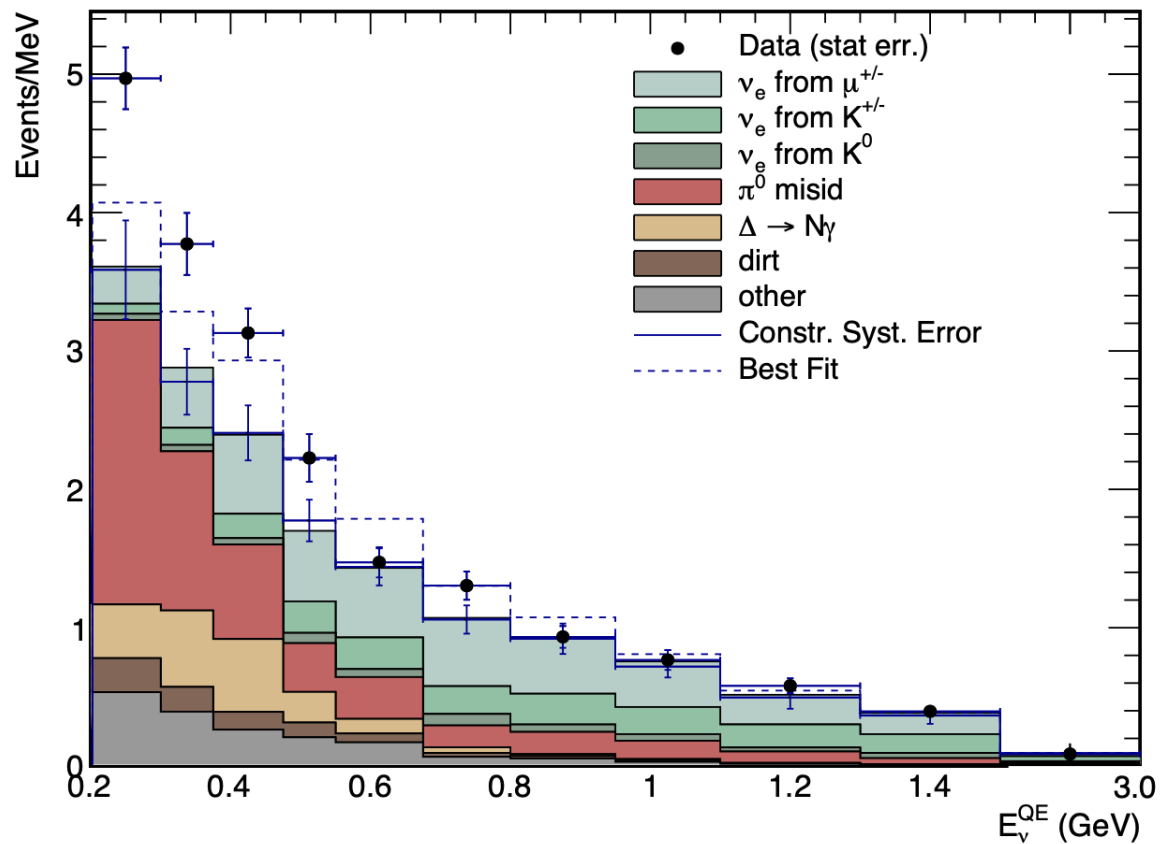
Why sterile neutrinos?

- All Standard Model (SM) neutrinos are left-handed, which do not have right-handed ones
- Right-handed neutrinos do not interact weakly, so-called "Sterile"

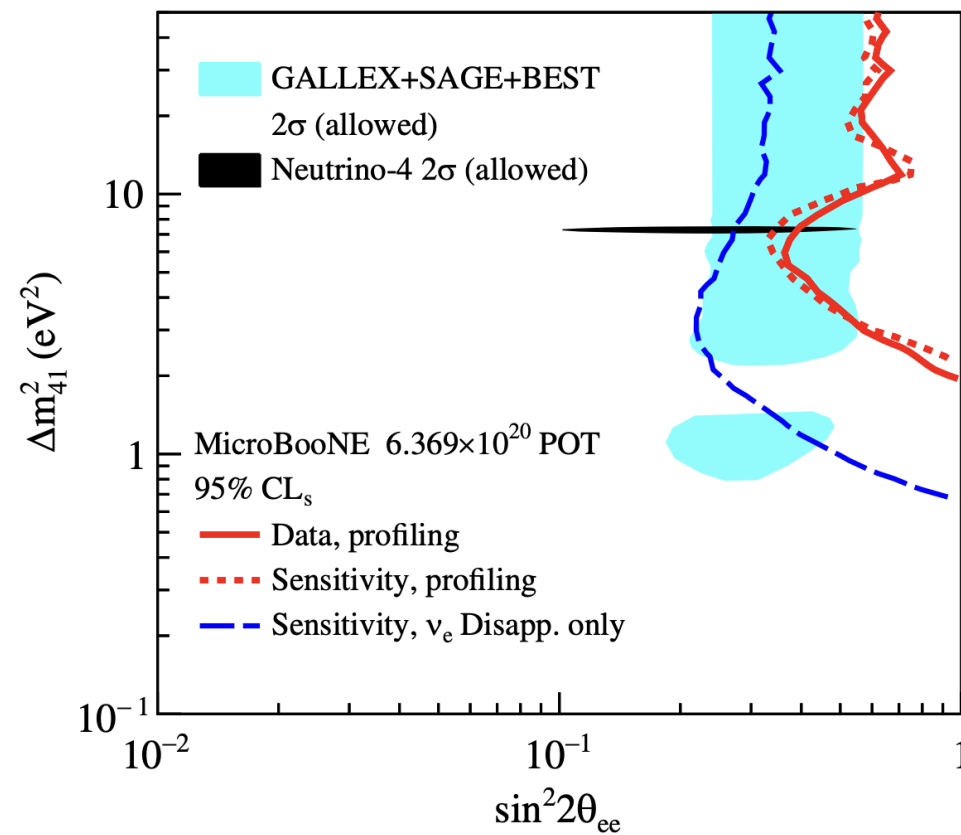


Short-baseline anomalies

Current constraints only provide the upper bound of light sterile neutrinos

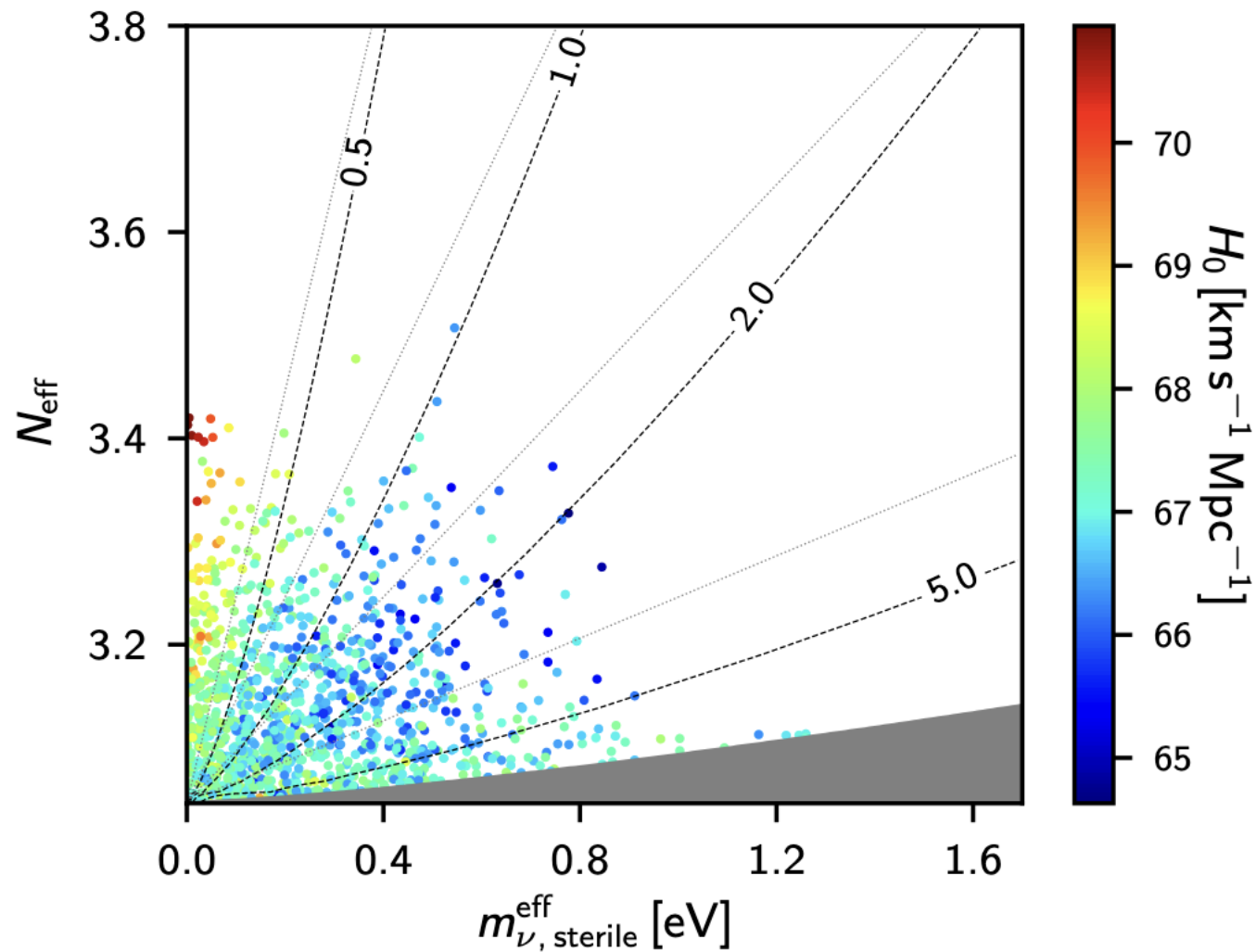


Excess of neutrino signatures (MiniBooNE, 2018)



Constraints (MicroBooNE, 2023)

Light sterile neutrino as dark radiation



Light Sterile Neutrinos(Planck, 2018)

$$\rho_{\text{rad}} = \left[\frac{7}{8} \left(\frac{4}{11} \right)^{4/3} N_{\text{eff}} \right] \rho_{\gamma}$$

$N_{\text{eff}} = 3.046$ counts for 3 types of neutrinos

For extra species, $\Delta N_{\text{eff}} \equiv N_{\text{eff}} - 3.046$

Notice: ΔN_{eff} is related to m_{phy} and mixing angle θ_{s*}

$$\left. \begin{array}{l} N_{\text{eff}} < 3.29, \\ m_{\nu, \text{sterile}}^{\text{eff}} < 0.65 \text{ eV}, \end{array} \right\} \begin{array}{l} 95 \%, \text{ Planck TT, TE, EE+lowE} \\ \text{+lensing+BAO,} \end{array}$$

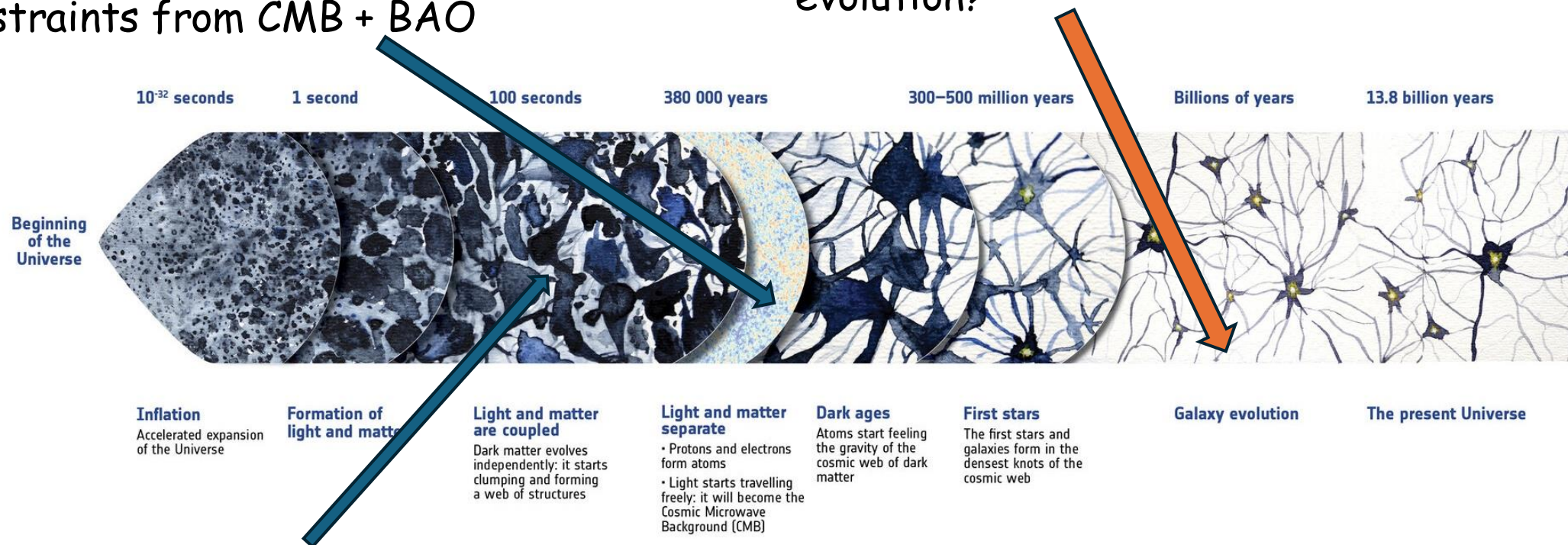
$$m_{\text{eff}} \equiv m_{\text{phy}} * \Delta N_{\text{eff}} \approx \Omega_{\nu_s} * 94.1 \text{ eV}$$

The sterile neutrino relics

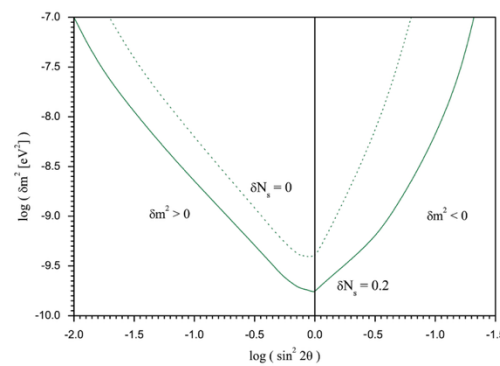
$$\left. \begin{array}{l} N_{\text{eff}} < 3.29, \\ m_{\nu, \text{sterile}}^{\text{eff}} < 0.65 \text{ eV}, \end{array} \right\} \begin{array}{l} 95 \%, \text{ Planck TT, TE, EE + lowE} \\ + \text{lensing + BAO}, \end{array}$$

Constraints from CMB + BAO

What can we learn about sterile neutrinos from the cosmological evolution?



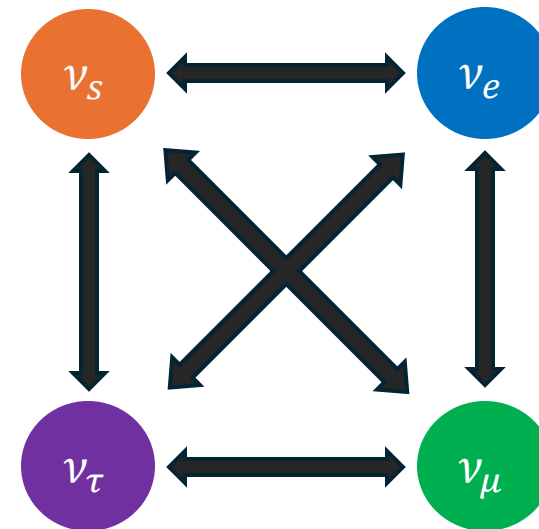
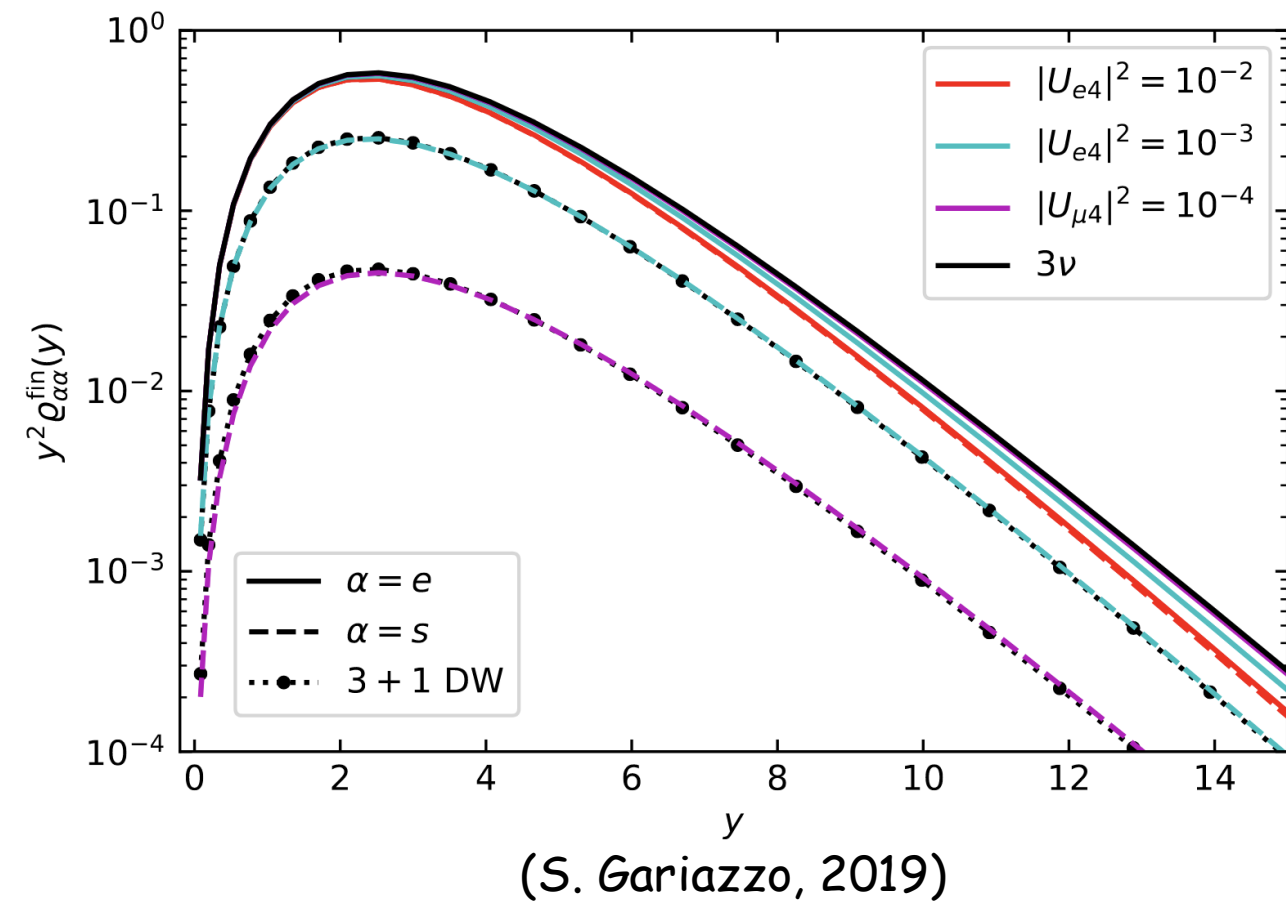
Constraints from BBN



Credit: EAS

(Mariana, 2024)

Neutrino Oscillation and Decoupling

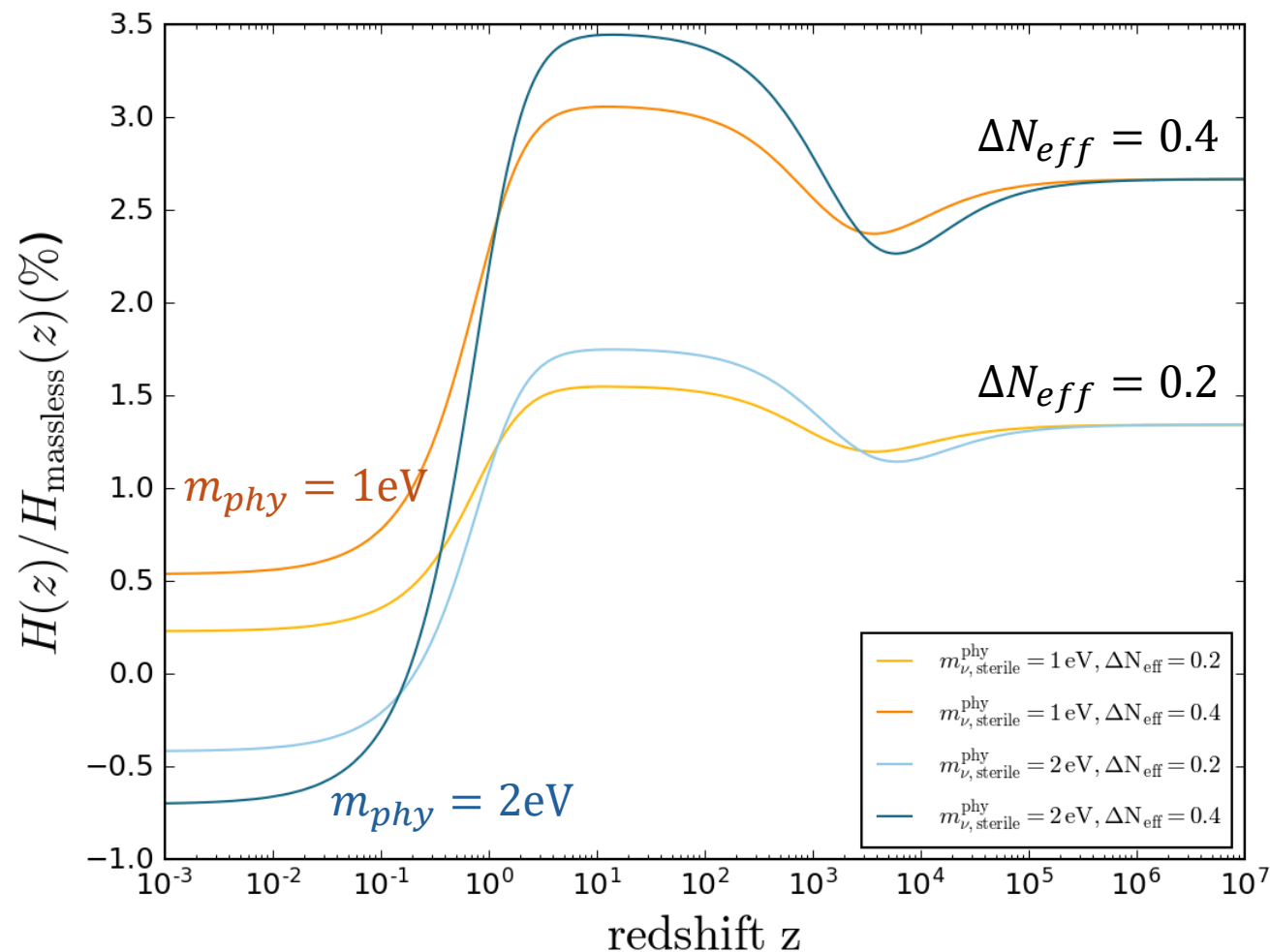


We assume sterile neutrinos are thermally produced by active-sterile neutrino oscillations

$$f_{\nu_s} = \Delta N_{\text{eff}} \frac{1}{e^{E/T} + 1}$$

Decoupled at $T \sim 1\text{MeV}$, so that $E \sim p$

The modified expansion rate of the universe



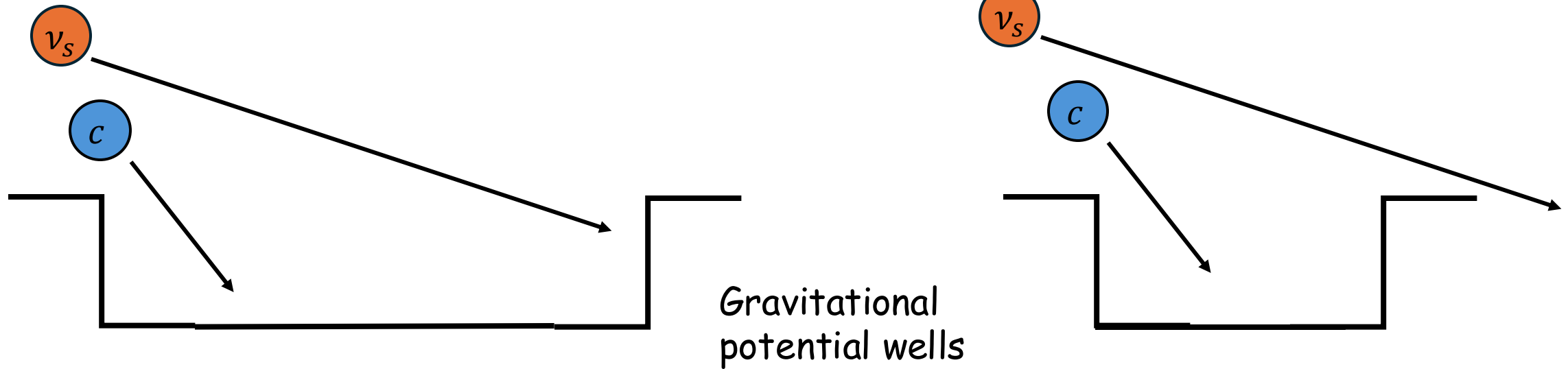
$$H(z) = H_0 \sqrt{\Omega_{\Lambda,0} + \Omega_{cb,0}a^{-3} + \Omega_{\gamma}a^{-4} + \frac{\rho_{\nu_a}(z)}{\rho_{cr}} + \frac{\rho_{\nu_s}(z)}{\rho_{cr}}}$$

- Fix cosmological parameter: $\{\Omega_{\Lambda}, \Omega_b, \Omega_m, \Omega_{\gamma}, H_0\}$
- Neutrinos are subtracted from CDM, so that $\Omega_m = \Omega_{\text{cdm}} + \Omega_b + \Omega_{\nu_a} + \Omega_{\nu_s}$ is fixed

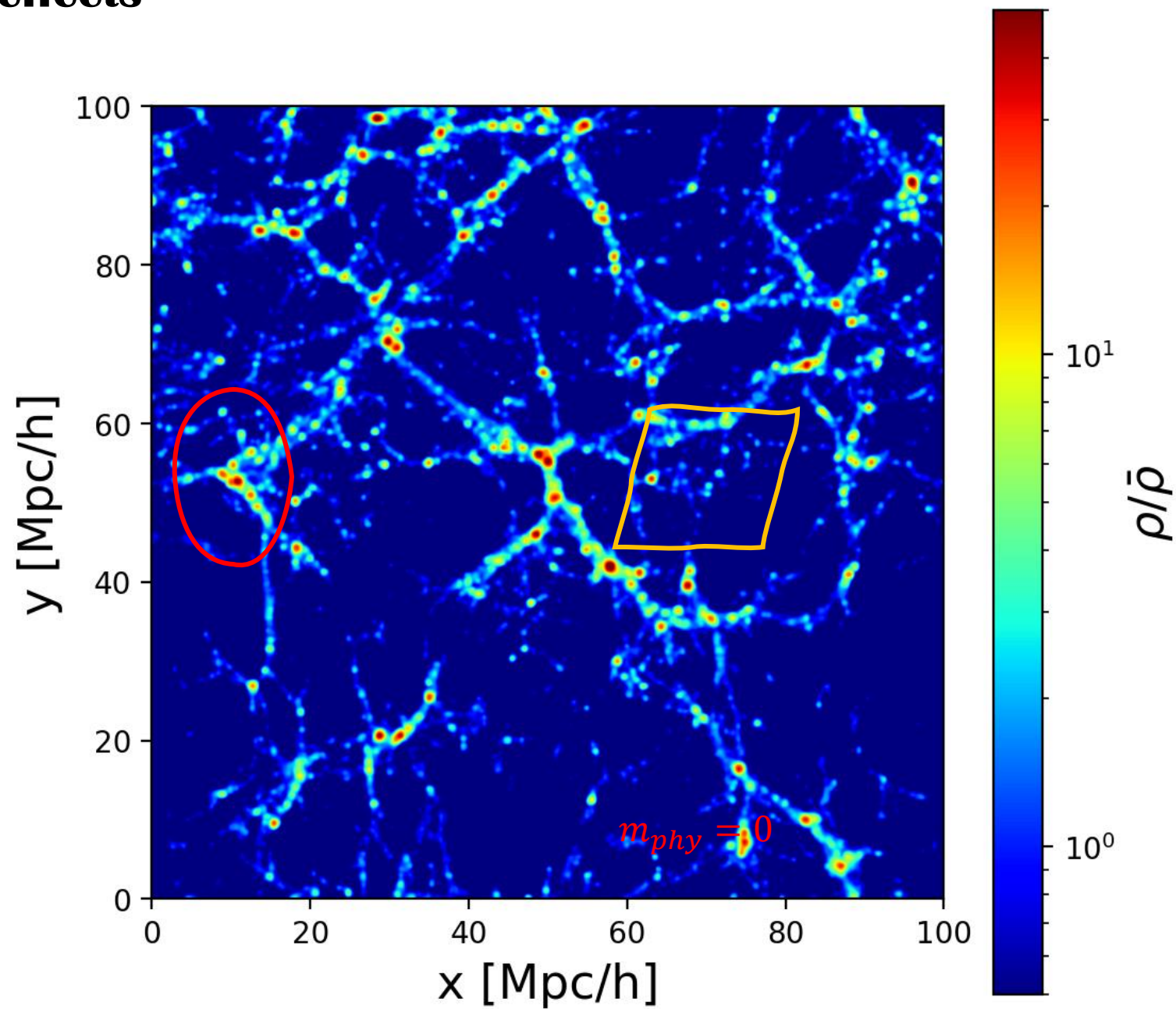
Free streaming effects

At low redshift, neutrinos become non-relativistic:

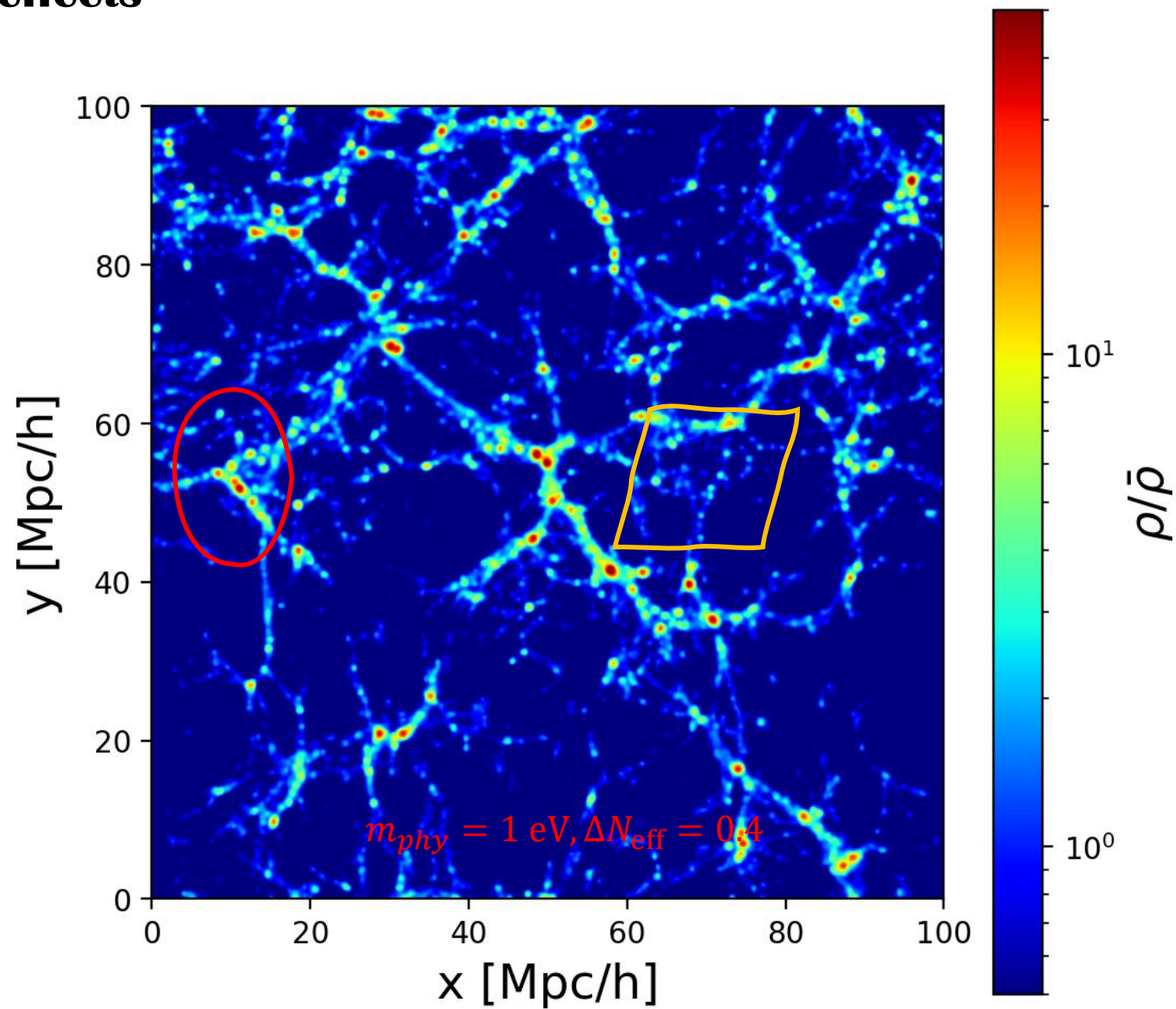
- But still have large thermal speed
→ smooth out the small structures.



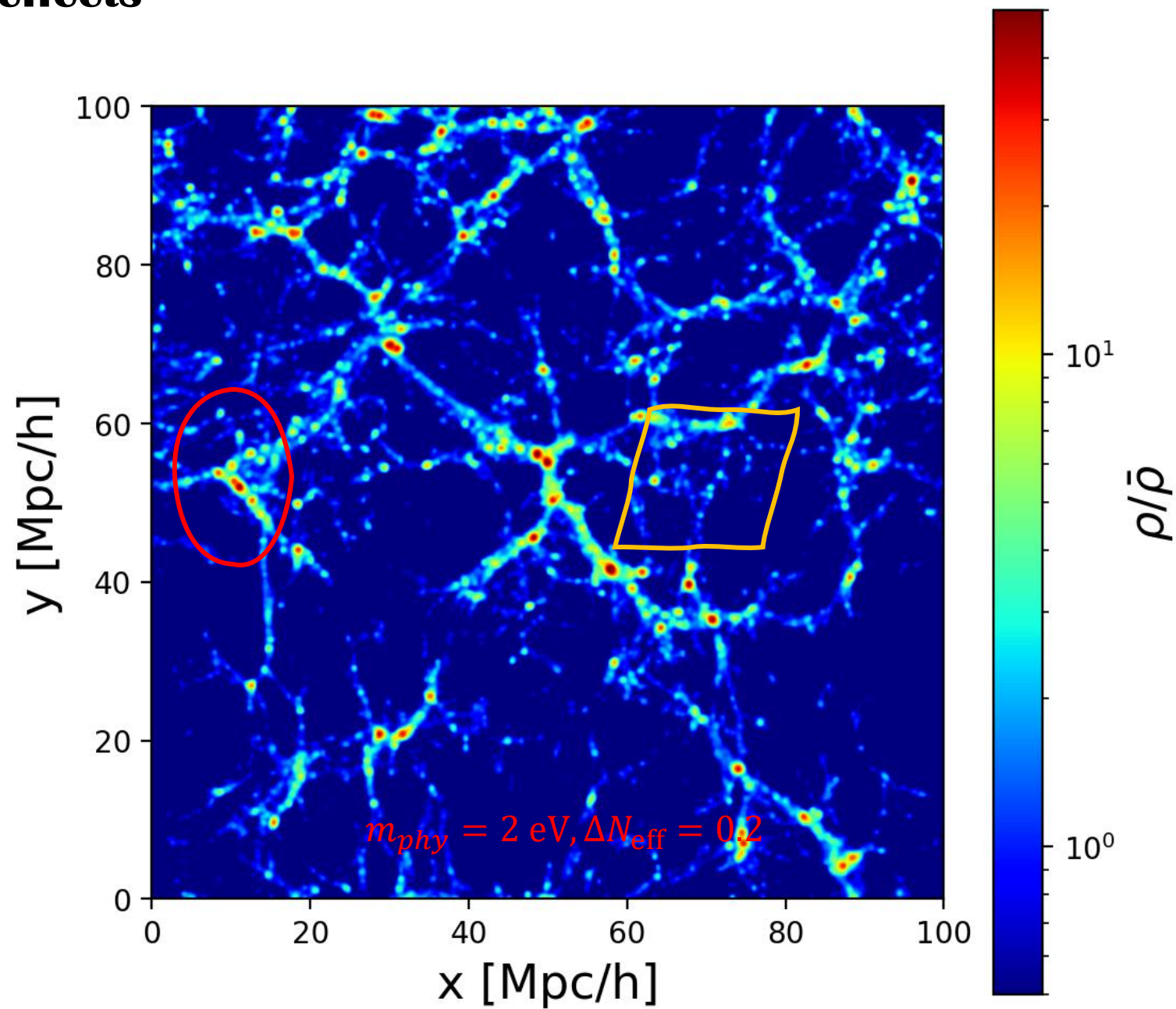
Free streaming effects



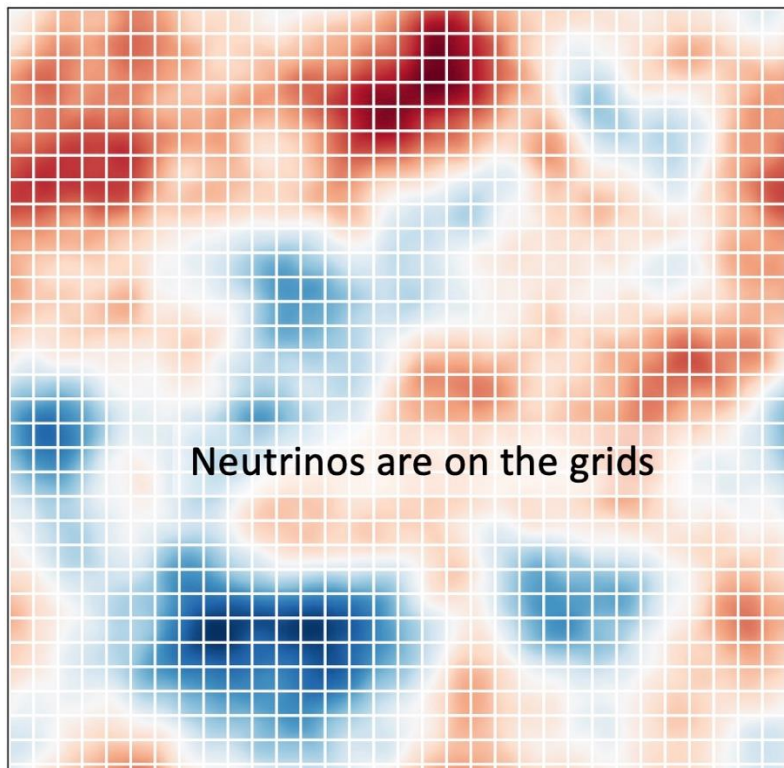
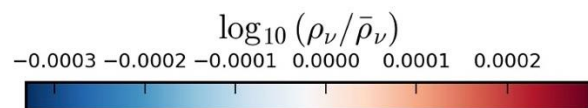
Free streaming effects



Free streaming effects



Linear response approach



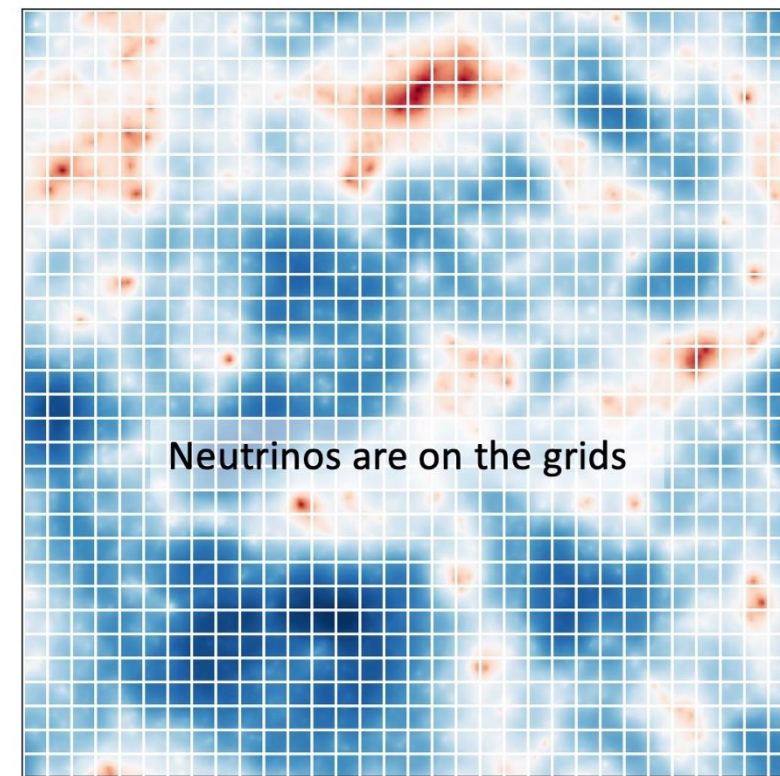
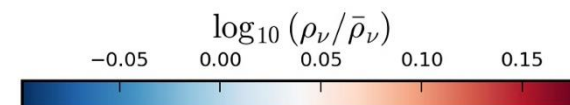
$z=49$

$$\delta_m = (1 - f_\nu)\delta_{cb} + f_\nu\delta_\nu$$

$$\frac{dF_{\nu_s}}{dt} = \frac{\partial F_{\nu_s}}{\partial t} + \frac{d\mathbf{r}}{dt} \cdot \frac{\partial F_{\nu_s}}{\partial \mathbf{r}} + \frac{d\mathbf{p}}{dt} \cdot \frac{\partial F_{\nu_s}}{\partial \mathbf{p}}$$

$$F_{\nu_s} = f_{\nu_s} + f'_{\nu_s}$$

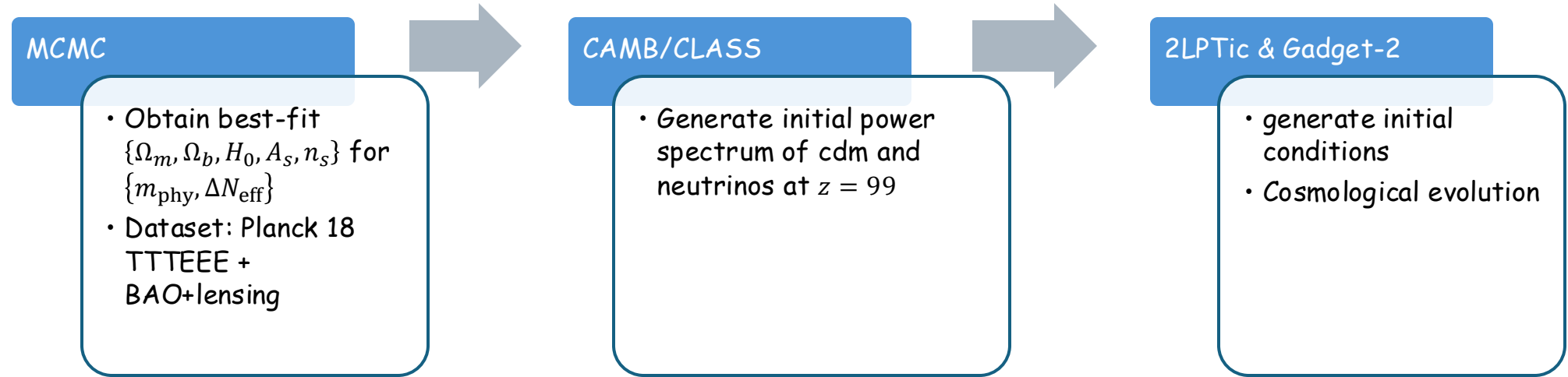
$\delta_{\nu_s}(k, t)$
 = (CDM potential)
 + (active neutrino potential) + (self
 – interaction)



$z=0$

Credit: Wangzheng

Simulation settings

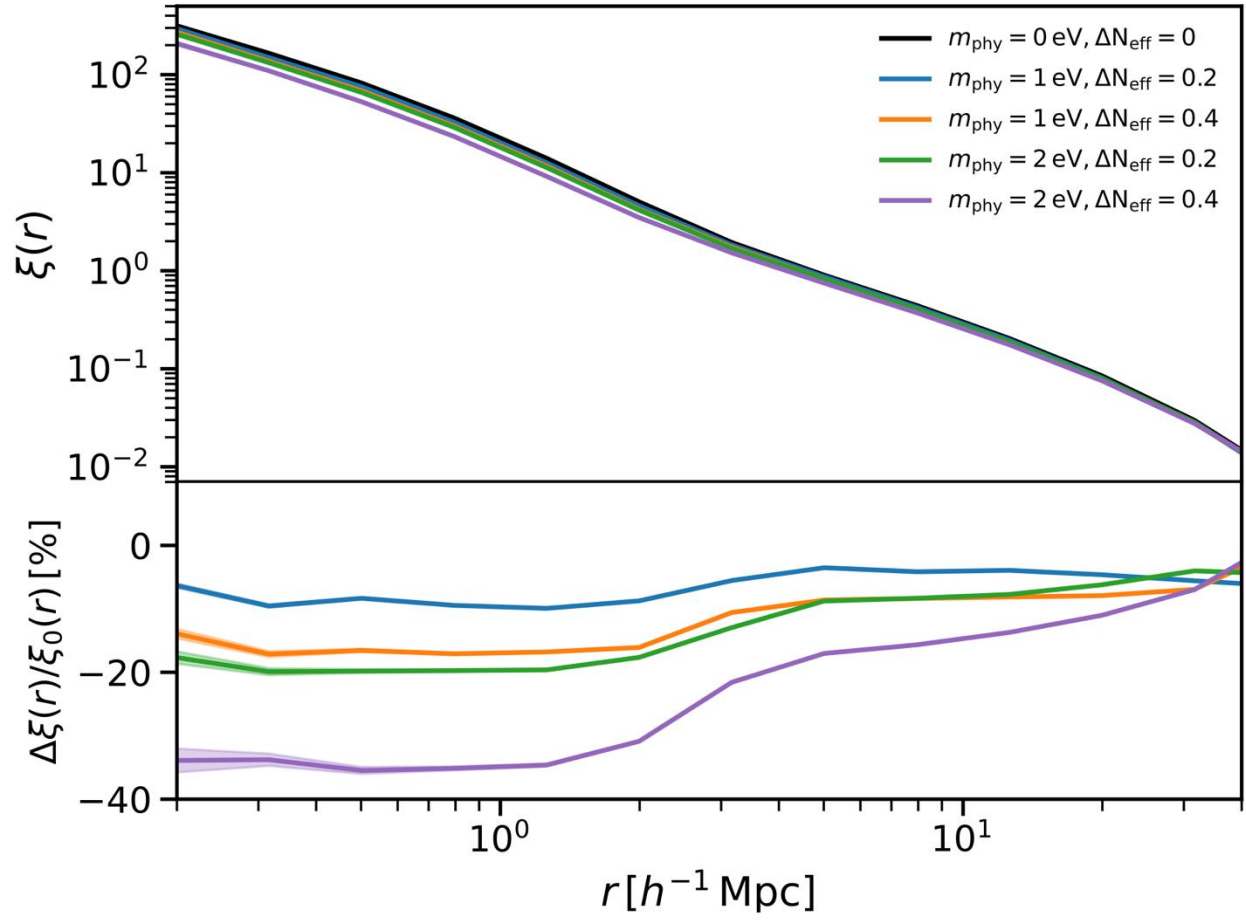
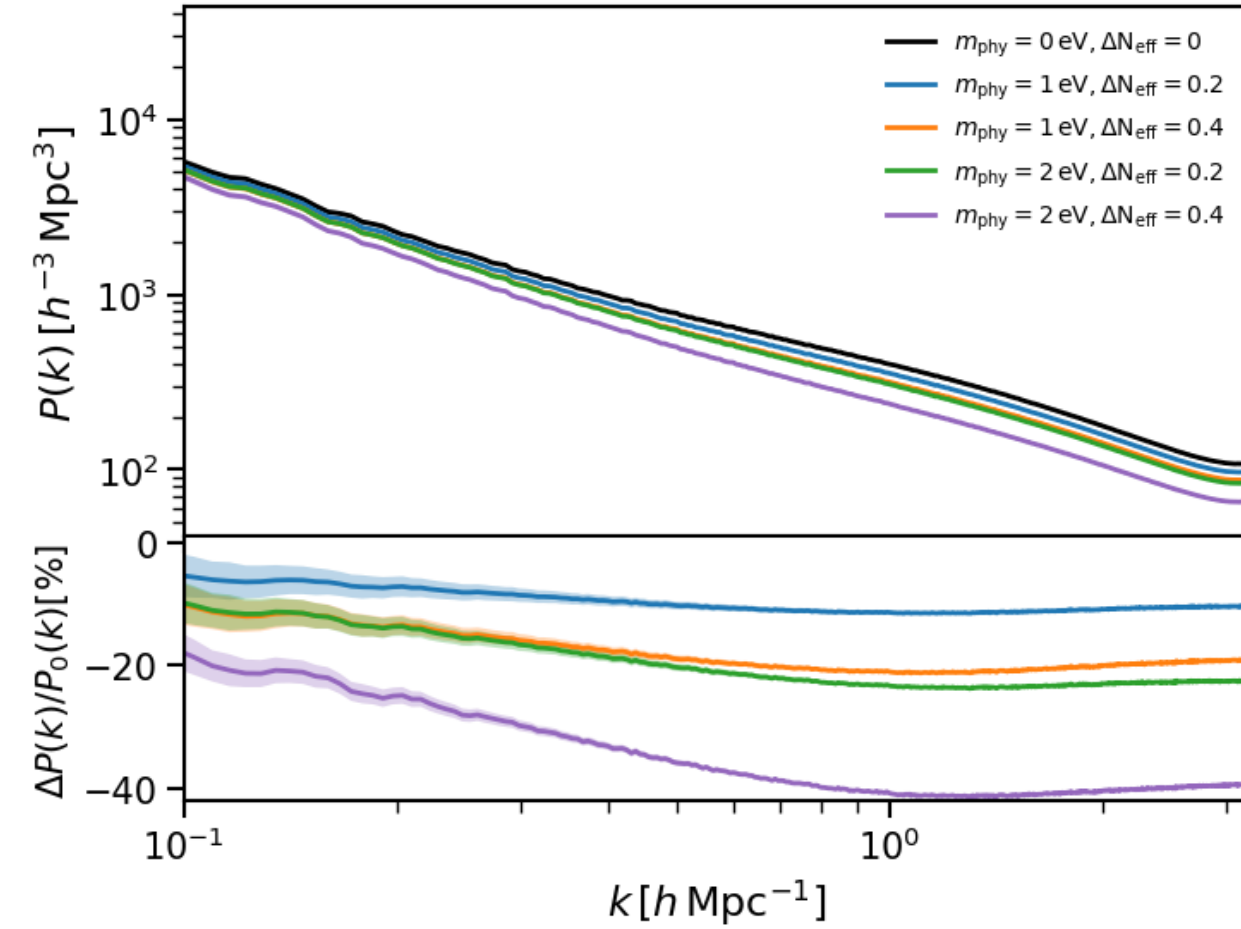


	$m_{\text{phy}} [\text{eV}]$	ΔN_{eff}	$H_0 [\text{km s}^{-1} \text{Mpc}^{-1}]$	$\Omega_c h^2$	$\Omega_b h^2$	Ω_Λ	n_s	$\ln A_s$
A0	0	0	67.75	0.1193	0.0224	0.6897	0.967	3.046
B1	1	0.2	67.90	0.1215	0.0226	0.6814	0.973	3.062
B2	1	0.4	68.11	0.1236	0.0228	0.6739	0.979	3.078
C1	2	0.2	67.46	0.1199	0.0226	0.6760	0.970	3.063
C2	2	0.4	67.27	0.1204	0.0228	0.6631	0.974	3.082

Have the same m_{eff}



Impact on matter field



$$R(m_{\text{phy}}, \Delta N_{\text{eff}}, k) \equiv \frac{\Delta P(k)}{P_0(k)} = \frac{P(m_{\text{phy}}, \Delta N_{\text{eff}}, k) - P(0 \text{ eV}, 0, k)}{P(0 \text{ eV}, 0, k)}$$

Impact on halo statistics

- We identified the distinct halos with at least one bounded halo located at the center as the main halo
- Halo mass M_{200c} : bounded mass within 200 times critical density

Halo mass function (HMF):

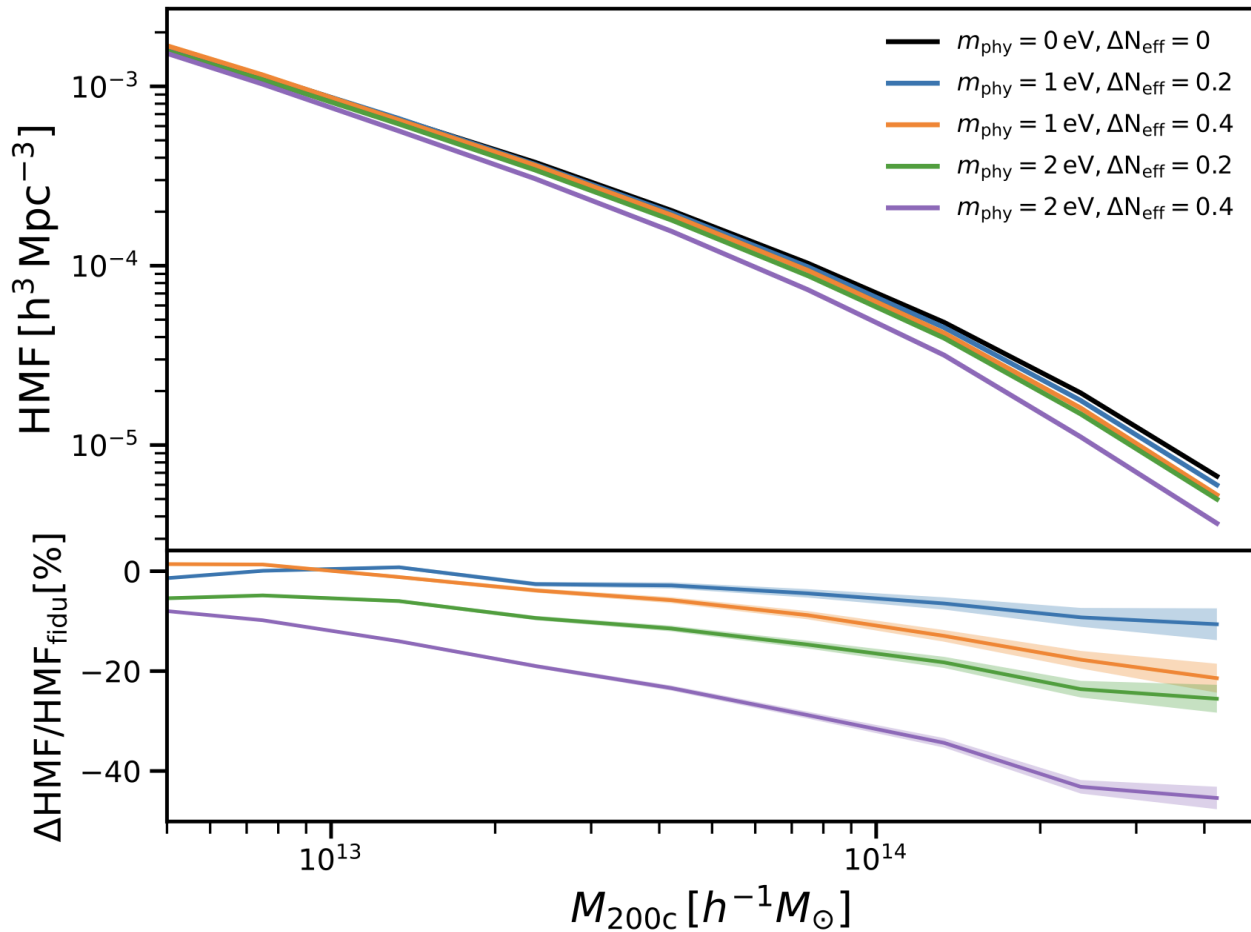
$$\text{HMF} \equiv \frac{dn}{d \log M_{200c}} = T(\sigma, z) \frac{\rho}{M_{200c}} \frac{d \log \sigma^{-1}(M, z)}{d \log M_{200c}}$$

$$\sigma^2 = \frac{1}{2\pi^2} \int_0^\infty k^2 P(k, z) W^2(k, R_{200c}) dk$$

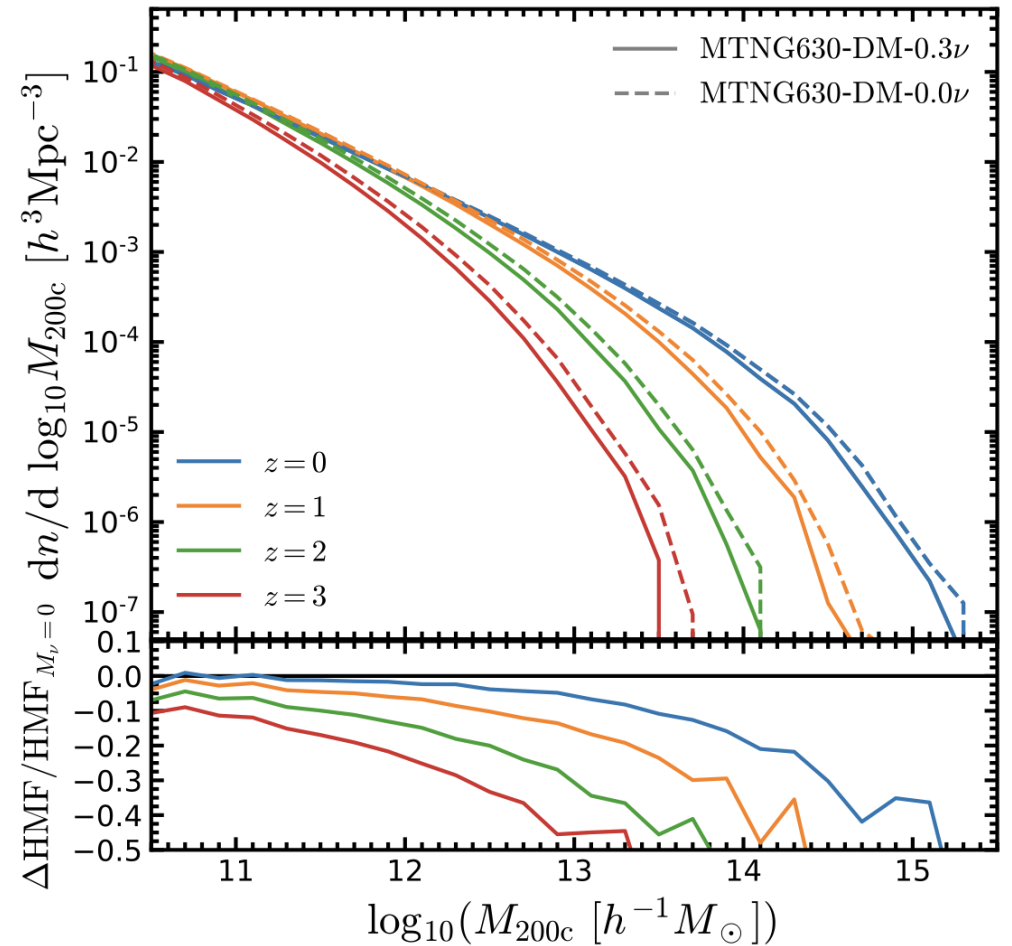
Maximum circular velocity function (HVF): $n_{>V}(V_{\text{circ}})$

$$V_{\text{circ}} \equiv \sqrt{\left. \frac{GM_{<r}}{r} \right|_{\text{Max}}}$$

Impact on halo statistics

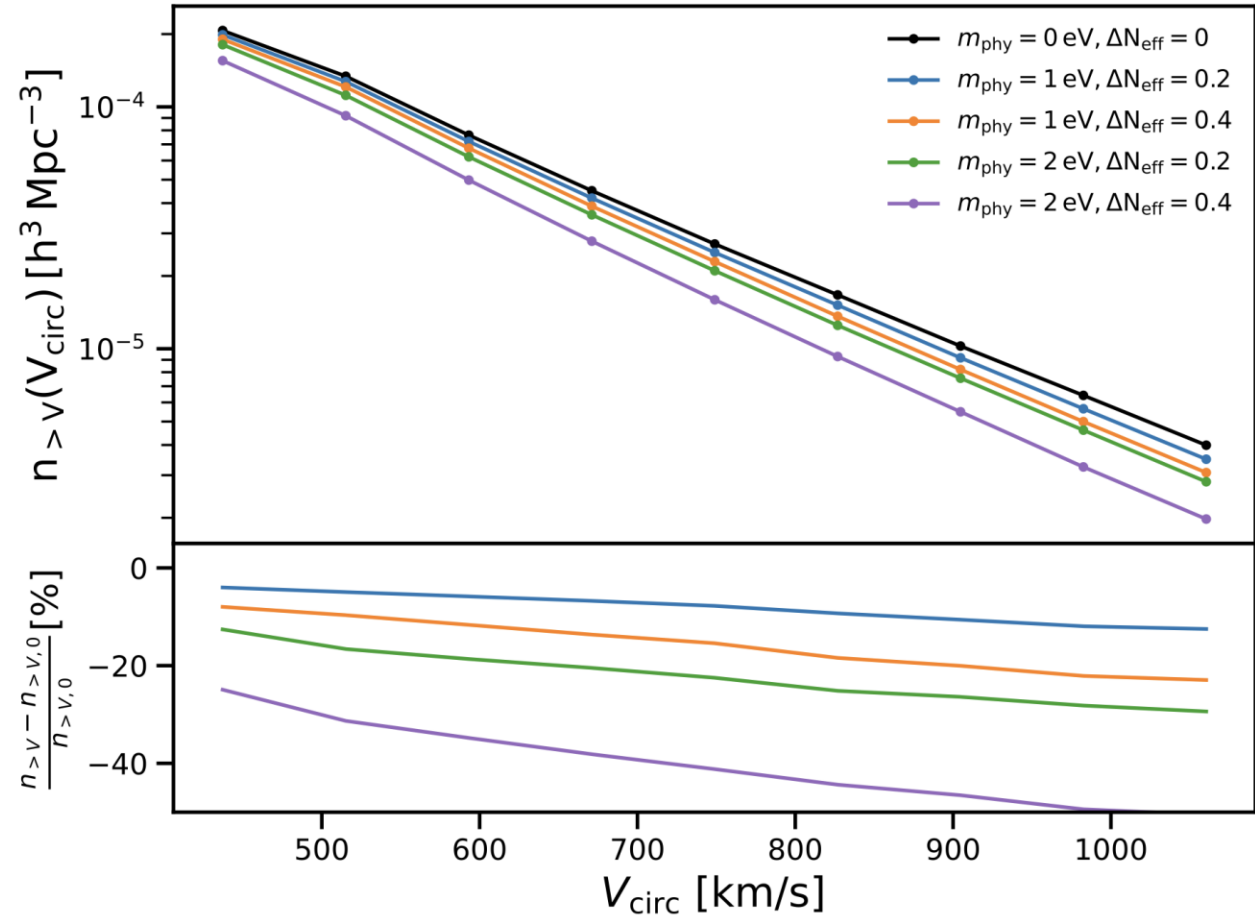
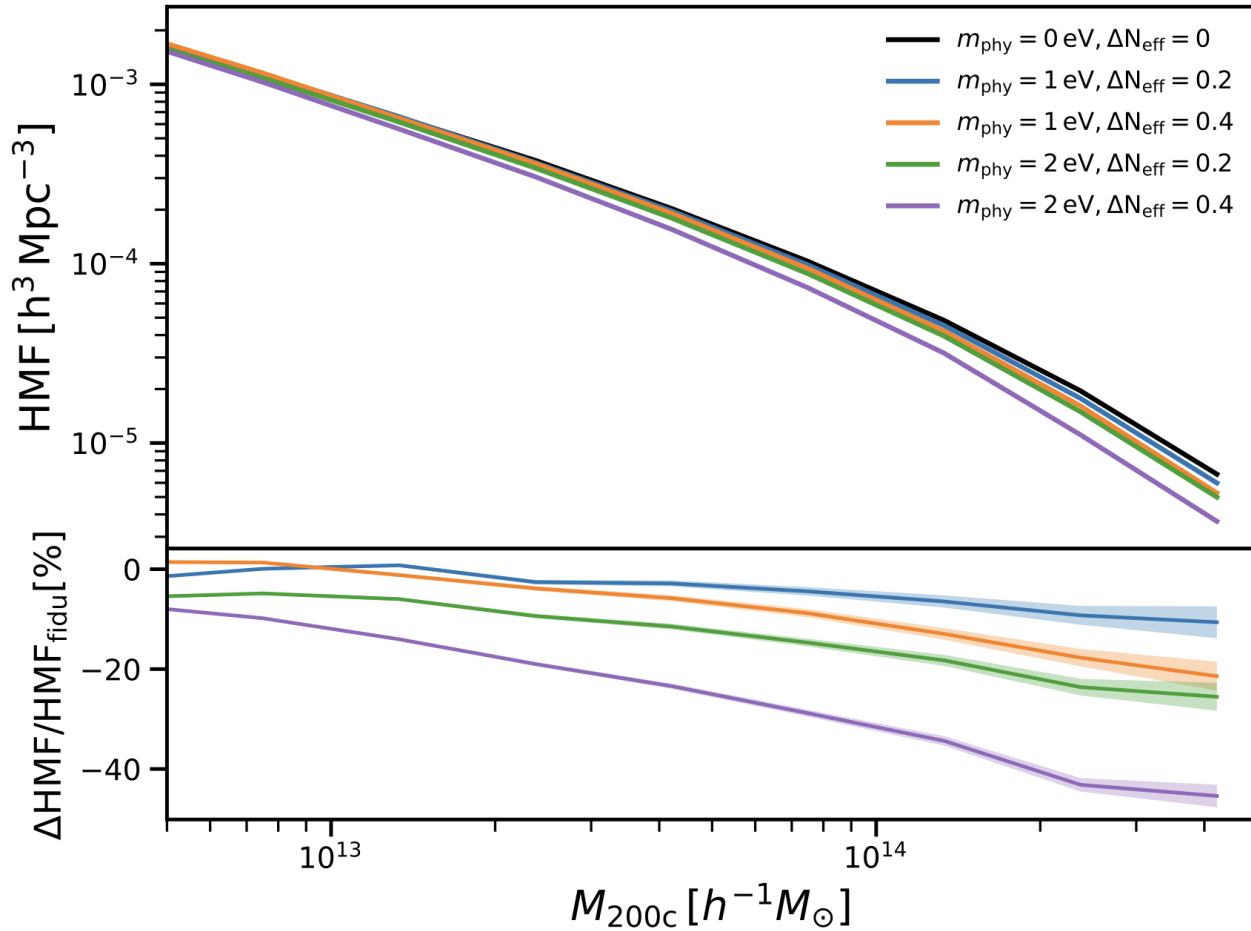


([MillenniumTNG, 2024](#))



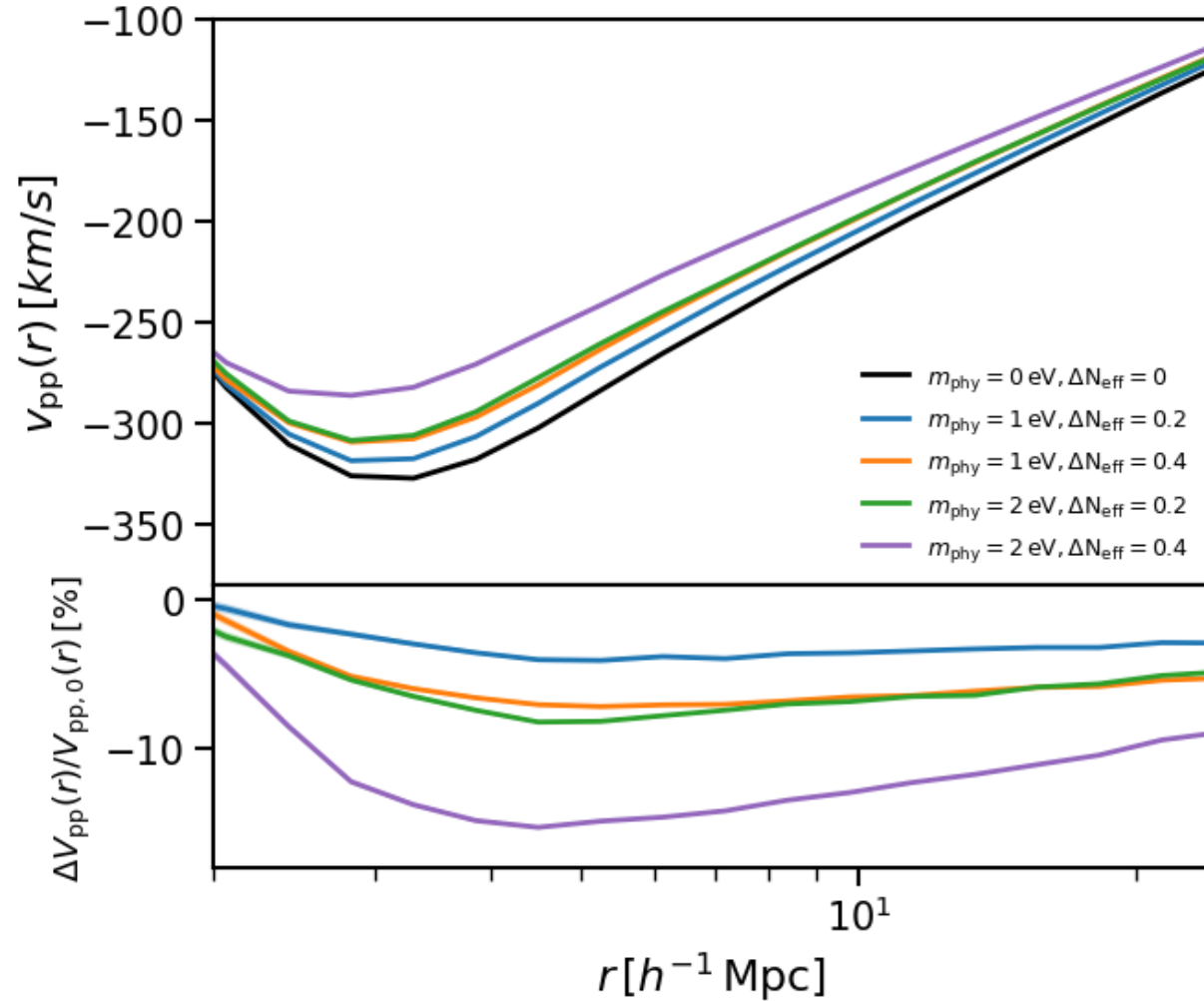
Sterile neutrinos may delay the halo formation, so halos with higher masses are less.

Impact on halo statistics

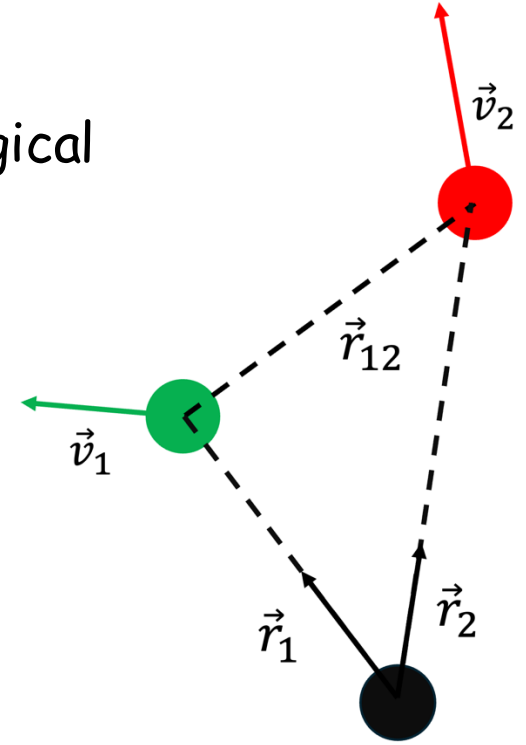


Sterile neutrinos may delay the halo formation, so halos with higher masses are less.

Peculiar motions



Velocity takes half of the information on the cosmological structures



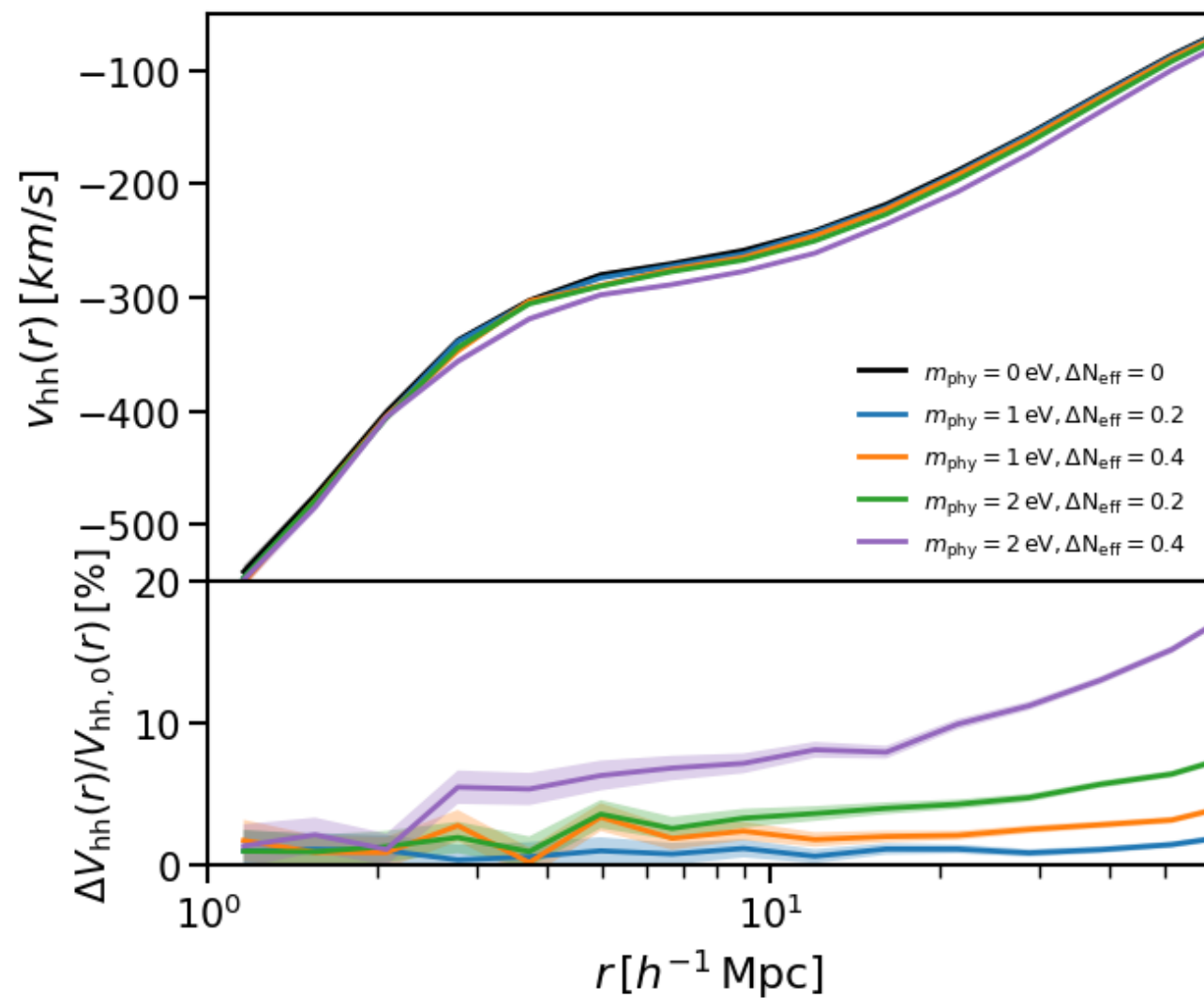
Pairwise velocity of object pairs:

$$v_{12}(r_{12}) \equiv \langle [\vec{v}_1(\vec{r}_1) - \vec{v}_2(\vec{r}_2)] \cdot \hat{r}_{12} \rangle$$

- $v_{12} < 0$, pairs tend to move towards each other
- r is large, pairs show little correlation, $v_{12} \rightarrow 0$

Impacts on pairwise velocity

For the halo mass range
 $M_h \in [10^{13}, 10^{14}] M_\odot h^{-1}$



Fittings of the impacts

For matter power spectrum:

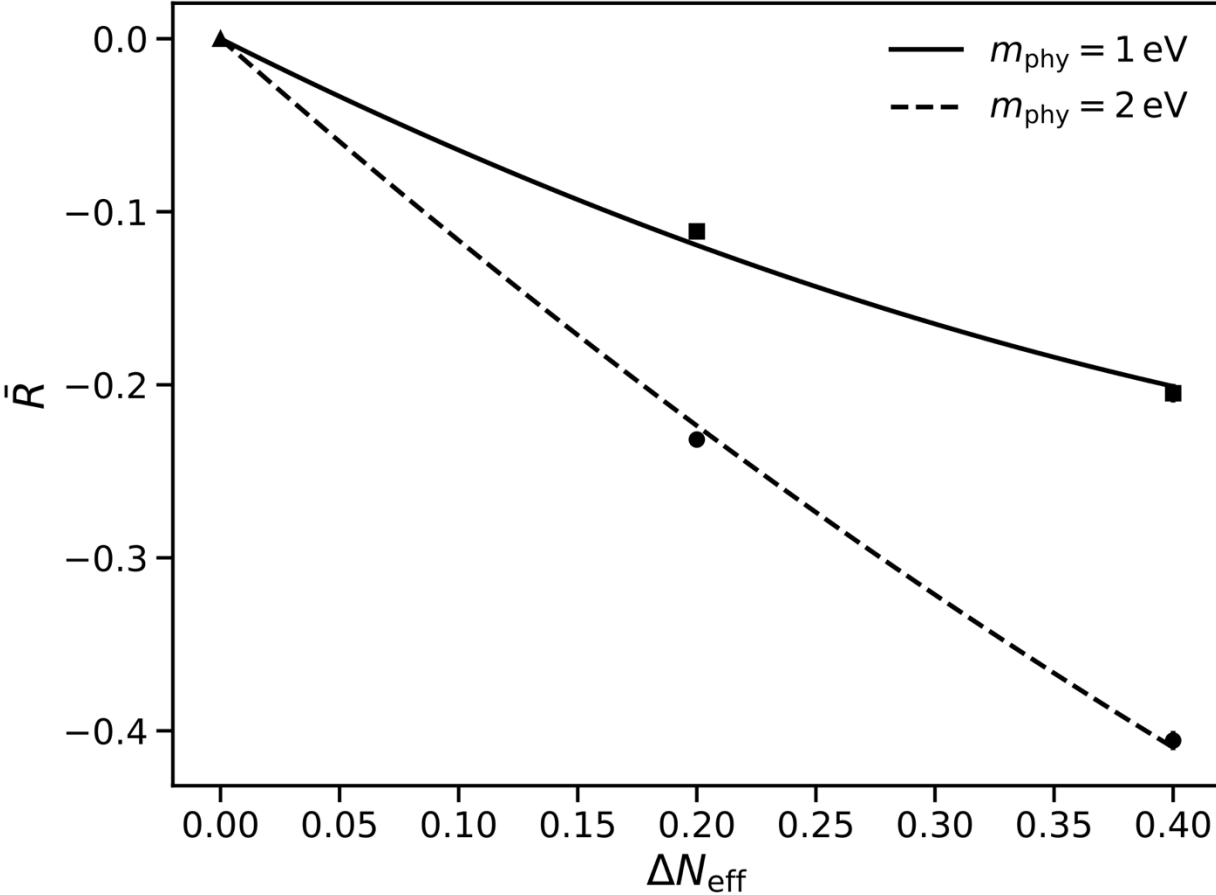
$$R(m_{\text{phy}}, \Delta N_{\text{eff}}, k) \equiv \frac{P(m_{\text{phy}}, \Delta N_{\text{eff}}, k) - P(m_{\text{phy}}, \Delta N_{\text{eff}}, k)}{P(0\text{eV}, 0, k)}$$

Perturbations on $\{m_{\text{phy}}, \Delta N_{\text{eff}}\} = \{0\text{eV}, 0\}$:

$$\begin{aligned} \bar{R}(m_{\text{phy}}, \Delta N_{\text{eff}}) &= C_{mm} \cdot \left(\frac{m_{\text{phy}}}{1\text{eV}}\right)^2 + C_{mn} \cdot \left(\frac{m_{\text{phy}}}{1\text{eV}}\right) \Delta N_{\text{eff}} + C_{nn} \\ &\cdot (\Delta N_{\text{eff}})^2 + C_m \cdot \left(\frac{m_{\text{phy}}}{1\text{eV}}\right) + C_n \cdot \Delta N_{\text{eff}} \end{aligned}$$

Table 3. Fitting results of \bar{R}_{hh}^v and $\bar{R}_{\text{hh}}^\sigma$ for $M_h \in [10^{13}, 10^{14}] M_\odot h^{-1}$ at the range $[6, 20] \text{Mpc } h^{-1}$.

quantity	$C_{nn}^{v/\sigma}$	$C_{mn}^{v/\sigma}$	$C_n^{v/\sigma}$
v_{hh}	0.034 ± 0.027	0.134 ± 0.006	-0.097 ± 0.012
σ_{hh}	0.041 ± 0.005	0.014 ± 0.001	-0.052 ± 0.002



\bar{R} : Averaged fractional deviations on $[0.7, 2.5] h \text{Mpc}^{-1}$



Check out neutrino cases (with chemical potential)!

Key Takeaways

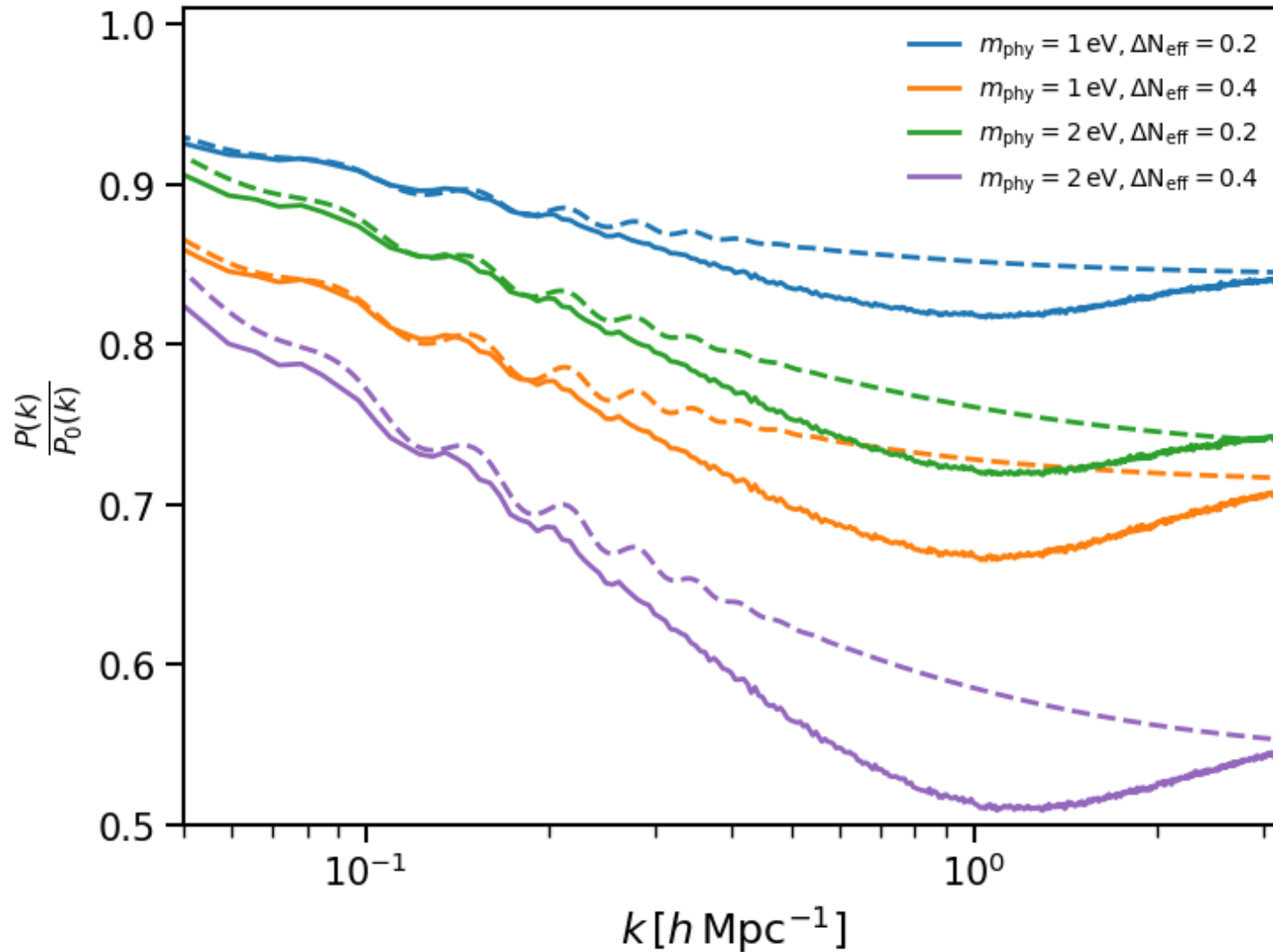
More details



JCAP06(2025)014

- Both matter PS and TPCF are suppressed by around 40% for $m_{\text{eff}} = 0.8\text{eV}$, with degeneracy between effects of m_{phy} and ΔN_{eff} broken for $k \geq 1 h \text{ Mpc}^{-1}$
- The presence of sterile neutrinos suppresses HMF and HVF by up to 40 – 50 % for $m_{\text{eff}} = 0.8 \text{ eV}$
- The halo-halo pairwise velocity increases in magnitude by up to 15% as m_{phy} or ΔN_{eff} increases for $M_h \in [10^{13}, 10^{14}] M_{\odot} h^{-1}$
- Future work could be utilize such observables with galaxy surveys to constrain sterile neutrino $\{m_{\text{phy}}, \Delta N_{\text{eff}}\}$

Appendix



- Compared with cosmology without sterile neutrinos
- Spoon-shaped deviation of power spectrum with fixed cosmologies for different $\{m_{phy}, \Delta N_{eff}\}$

Appendix

Combining Eq. (A.2), the Friedmann equation, and Eq. (A.3), Eq. (A.5) can be linearized as

$$\frac{\partial f_{\nu_s}^1}{\partial s} + \mathbf{u} \cdot \frac{\partial f_{\nu_s}^1}{\partial \mathbf{x}} - Ga^4 \frac{\partial f_{\nu_s}^0}{\partial \mathbf{u}} \cdot \int \bar{\rho}_t \delta_t(s, \mathbf{x}') \frac{\mathbf{x} - \mathbf{x}'}{|\mathbf{x} - \mathbf{x}'|^3} d^3 \mathbf{x}', \quad (\text{A.6})$$

where $\bar{\rho}_t \delta_t \equiv \rho_t - \bar{\rho}_t = \bar{\rho}_{cb} \delta_{cb} + \bar{\rho}_\nu \delta_\nu$. By applying the Fourier transformation and integrating out s from initial time s_i , one can obtain

$$\begin{aligned} \tilde{f}_{\nu_s}^1(s, \mathbf{k}, \mathbf{u}) + \int_{s_i}^s e^{-i\mathbf{k} \cdot \mathbf{u}(s-s')} 4\pi Ga^4 \frac{i\mathbf{k}}{k^2} \frac{f_{\nu_s}^0}{\partial \mathbf{u}} \left[\bar{\rho}_{cb}(s') \tilde{\delta}_{cb}(s', \mathbf{k}) + \bar{\rho}_\nu(s') \tilde{\delta}_\nu(s', \mathbf{k}) \right] ds' = \\ \tilde{f}_{\nu_s}^1(s, \mathbf{k}, \mathbf{u}) e^{-i\mathbf{k} \cdot \mathbf{u}(s-s_i)}, \end{aligned} \quad (\text{A.7})$$

Appendix

where ' \sim ' denotes the corresponding Fourier transformed variables. Following Ali-Haimoud's work [23], the initial $\tilde{f}_{\nu_s}^1(s_i, \mathbf{k}, \mathbf{u})$ can be expanded by Legendre polynomials

$$\tilde{f}_{\nu_s}^1(s_i, \mathbf{k}, \mathbf{u}) = \sum_{l=0}^{\infty} i^l \tilde{f}_{\nu_s}^{1,(l)}(s_i, \mathbf{k}, \mathbf{u}) P_l(\hat{\mathbf{k}} \cdot \hat{\mathbf{u}}), \quad (\text{A.8})$$

with the coefficients approximated as

$$\begin{aligned} \tilde{f}_{\nu_s}^{1,(0)} &= f_{\nu_s}^0 \tilde{\delta}_{\nu_s}(s_i, \mathbf{k}), \\ \tilde{f}_{\nu_s}^{1,(1)} &= \frac{df_{\nu_s}^0(u)}{du} k^{-1} a_i \tilde{\theta}_{\nu_s}(s_i, \mathbf{k}) = -\frac{df_{\nu_s}^0(u)}{du} k^{-1} a_i^2 H(a_i) \tilde{\delta}_{\nu_s}(s_i, \mathbf{k}), \\ \tilde{f}_{\nu_s}^{1,(l)} &= 0 (l \geq 2), \end{aligned} \quad (\text{A.9})$$

$$\begin{aligned} \tilde{\delta}_{\nu_s} &= \tilde{\delta}_{\nu_s}(s_i, \mathbf{k}) \Phi[\mathbf{k}(s - s_i)] [1 + (s - s_i) a_i^2 H(a_i)] + 4\pi G \int_{s_i}^s a^4(s - s') \Phi[\mathbf{k}(s - s')] \\ &\quad \times \left[\bar{\rho}_{cb}(s') \delta_{cb}(s', \mathbf{k}) + \sum_i \bar{\rho}_{\nu_i}(s') \delta_{\nu_i}(s', \mathbf{k}) + \bar{\rho}_{\nu_s}(s') \delta_{\nu_s}(s', \mathbf{k}) \right] ds', \end{aligned}$$

where $\Phi(\mathbf{q}) \equiv \frac{\int f_{\nu_s}^0 e^{-i\mathbf{q} \cdot \mathbf{u}} d^3\mathbf{u}}{\int f_{\nu_s}^0 d^3\mathbf{u}}.$

Appendix

